Bistable regimes in an optically injected mode-locked laser

Tatiana Habruseva,[1,4,*] **Stephen P. Hegarty,**[1,4]
Andrei G. Vladimirov,[1,2] **Alexander Pimenov,**[2] **Dmitrii Rachinskii,**[3]
Natalia Rebrova,[1,4] **Evgeny A. Viktorov,**[4] **and Guillaume Huyet**[1,4]

[1]*Center of Advanced Photonics and Process Analysis, Cork Institute of Technology, Ireland*
[2]*Weierstrass Institute, Berlin, Germany*
[3]*University College Cork, Cork, Ireland*
[4]*Tyndall National Institute, Cork, Ireland*
[*]*tatiana.gabruseva@gmail.com*

Abstract: We study experimentally the dynamics of quantum-dot (QD) passively mode-locked semiconductor lasers under external optical injection. The lasers demonstrated multiple dynamical states, with bifurcation boundaries that depended upon the sign of detuning variation. The area of the hysteresis loops grew monotonically at small powers of optical injection and saturated at moderate powers. At high injection levels the hysteresis decreased and eventually disappeared.

OCIS codes: (140.0140) Lasers and laser optics; (140.4050) Mode-locked lasers; (190.1450) Bistability; (250.5590) Quantum-well, -wire and -dot devices.

References and links

1. J. Ye, and S. Cundiff, *Femtosecond Optical Frequency Comb: Principle, Operation, and Applications* (Springer Berlin, 2004).
2. P. J. Delfyett, S. Gee, M.-T. Choi, H. Izadpanah, W. Lee, S. Ozharar, F. Quinlan, and T. Yilmaz, "Optical frequency combs from semiconductor lasers and applications in ultrawideband signal processing and communications," J. Lightwave Technol. **24**, 2701–2719 (2006).
3. E. U. Rafailov, M. A. Cataluna, and W. Sibbett, "Mode-locked quantum-dot lasers," Nat. Photonics **1**, 395–401 (2007).
4. E. A. Viktorov, P. Mandel, M. Kuntz, G. Fiol, D. Bimberg, A. G. Vladimirov, and M. Wolfrum, "Stability of the mode-locked regime in quantum dot lasers," Appl. Phys. Lett. **91**, 231116 (2007).
5. M. Feng, S. T. Cundiff, R. P. Mirin, and K. L. Silverman, "Wavelength bistability and switching in two-section quantum-dot diode lasers," IEEE J. Quantum Electron. **46**, 951–958 (2010).
6. K. Silverman, M. Feng, R. Mirin, and S. Cundiff, "Exotic behavior in quantum dot mode-locked lasers: dark pulses and bistability," in *Quantum Dot Devices, Lecture Notes in Nanoscale Science and Technology* **13** (Springer-Verlag, NY, 2012) pp. 23–48.
7. T. Habruseva, S. O'Donoghue, N. Rebrova, D. A. Reid, L. Barry, D. Rachinskii, G. Huyet, and S. P. Hegarty, "Quantum-dot mode-locked lasers with dual-mode optical injection," IEEE Photon. Technol. Lett. **22**(6), 359–361 (2010).
8. N. Rebrova, T. Habruseva, G. Huyet, and S. P. Hegarty, "Stabilization of a passively mode-locked laser by continuous wave optical injection," Appl. Phys. Lett. **97**, 101105 (2010).
9. G. Fiol, D. Arsenijevic, D. Bimberg, A. G. Vladimirov, M. Wolfrum, E. A. Viktorov, and P. Mandel, "Hybrid mode-locking in a 40 GHz monolithic quantum dot laser," Appl. Phys. Lett. **96**, 011104 (2010).
10. N. Rebrova, G. Huyet, D. Rachinskii, and A. G. Vladimirov, "Optically injected mode-locked laser," Phys. Rev. E **83**, 066202 (2011).
11. M. Todaro, J. Tourrenc, S. P. Hegarty, C. Kelleher, B. Corbett, G. Huyet, and J. G. McInerney, "Simultaneous achievement of narrow pulse width and low pulse-to-pulse timing jitter in 1.3 μm passively mode-locked quantum-dot lasers," Opt. Lett. **31**, 3107–3109 (2006).
12. T. Habruseva, S. O'Donoghue, N. Rebrova, S. P. Hegarty, and G. Huyet, "Quantum-dot mode-locked lasers with optical injection," SPIE Proceedings **7608**, 760803 (2010).

#173554 - $15.00 USD Received 2 Aug 2012; revised 28 Sep 2012; accepted 3 Oct 2012; published 25 Oct 2012

13. T. Habruseva, N. Rebrova, S. P. Hegarty, and G. Huyet, "Mode-locked semiconductor lasers with optical injection," in *Quantum Dot Devices, Lecture Notes in Nanoscale Science and Technology*, **13** Springer-Verlag, NY, 2012) pp. 65–91.
14. P. M. Varangis, A. Gavrielides, T. Erneux, V. Kovanis, and L. F. Lester, "Frequency entrainment in optically injected semiconductor lasers," Phys. Rev. Lett. **78**, 2353–2356 (1997).
15. T. B. Simpson, "Mapping the nonlinear dynamics of a distributed feedback semiconductor laser subject to external optical injection," Opt. Commun. **215**, 135–151 (2003).
16. P. A. Braza, and T. Erneux, "Constant phase, phase drift, and phase entrainment in lasers with an injected signal," Phys. Rev. A **41**, 6470–6479 (1990).
17. B. Kelleher, D. Goulding, B. B. Pascual, S. P. Hegarty, and G. Huyet, "Bounded phase phenomena in the optically injected laser," Phys. Rev. E **85**, 046212 (2012).
18. A. Pikovsky, M. Rosenblum, and J. Kurths, "Synchronization. A universal concept in nonlinear sciences" (Cambridge University Press 2001).
19. T. Erneux, E. A. Viktorov, B. Kelleher, D. Goulding, S. P. Hegarty, and G. Huyet, "Optically injected quantum dot lasers," Opt. Lett. **35**, 937–939 (2010).
20. J. K. White, J. V. Moloney, A. Gavrielides, V. Kovanis, A. Hohl, and R. Kalmus, "Multilongitudinal-mode dynamics in a semiconductor laser subject to optical injection," IEEE J. Quantum. Elecron. **34**, 1469–1473 (1998).

1. Introduction

Optical frequency combs are important for a number of applications including time and frequency metrology [1], arbitrary waveform generation, coherent communications and signal processing [2]. These combs are commonly generated by mode-locked lasers (MLLs) that periodically emit short pulses with an optical spectrum composed of a set of equally spaced narrow linewidth frequencies. Mode-locked lasers based on quantum dot (QD) semiconductor materials are of particular interest due to their broadband gain and fast carrier dynamics [3]. These lasers possess a rich diversity of dynamical regimes [4] including lasing wavelength bistability and hysteresis under variation of the reverse bias voltage [5, 6]. These regimes can potentially be exploited for high speed switching or data storage in optical networks. Recent experiments on optical injection locking of QD-MLLs have shown an improved control of the pulse train, chirp reduction, wavelength tuning, and pulse stabilization [7, 8]. A number of theoretical studies revealed the bifurcation mechanisms responsible for phase locking of a MLL to an external master frequency and pulse repetition frequency locking of a hybrid MLL to external RF modulation [8–10].

In this work we study the complex dynamical regimes and bifurcation phenomena of QD-MLLs injected by a master laser. Using two-section QD-MLLs subject to a narrow linewidth optical injection, we experimentally identify the different dynamical states of operation, their locking boundaries and the multiple bistabilities of the system.

2. Experimental setup

In the experiments, the slave laser was an uncoated two-section monolithic InAs/GaAs QD-MLL, similar to that described in [11], emitting at 1.3 μm with a repetition rate of 10.3 GHz. The device (20% absorber section) was mounted on a temperature controlled stage at room temperature, an enclosure was used to exclude draughts and reduce temperature fluctuations to the order of 10 mK. The absorber bias was -2.0 V for the experiments described here, with a laser threshold of 157 mA at -2.0 V. The master laser was a commercial external cavity tunable laser source (TLS, Agilent 81672 B) with a linewidth of $\sim$ 200 kHz. The master light was injected through a polarization maintaining (PM) fibre circulator and coupled to the slave gain section via a PM lens fibre. The experimental setup is shown in Fig. 1. The slave laser output was measured using optical and electrical spectrum analyzers, a power meter, an autocorrelator (Fig. 1(a)), and a linear pulse recovery instrument (frequency-resolved Mach-Zehnder gating, Southern Photonics EG130, Fig. 1(b)) [7]. The optical linewidth of slave individual modes was

#173554 - $15.00 USD Received 2 Aug 2012; revised 28 Sep 2012; accepted 3 Oct 2012; published 25 Oct 2012

measured through heterodyne beating of the slave modes with a tunable laser source TLS 2 having a narrow linewidth of $\sim$ 200 kHz as shown in Fig. 1(c).

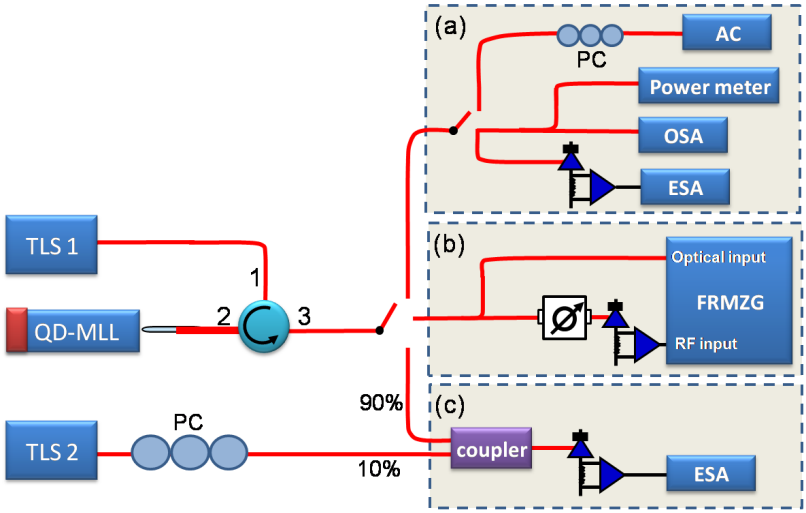

Fig. 1. Schematic of the experimental setup for characterization of the QD-MLL under external optical injection. TLS: tunable laser source; PC: polarization controller; AC: autocorrelator; OSA: optical spectrum analyzer; ESA: electronic spectrum analyzer; FRMZG: frequency-resolved Mach-Zehnder gating.

For characterization of optically injected QD-MLL dynamics we varied the detuning Δ between master and slave, $\Delta = \omega_m - \omega_s$, and measured the average power and the optical and electronic spectra of the slave for each value of the detuning. Tuning steps of our TLS were only possible in a non-monotonic "overshoot-return" manner, unusable for characterization of hysteresis phenomena. To ensure continuous scanning of Δ, the master frequency ω_m was fixed and monotonic steps in the slave laser current were made, with the current step starting from 0.01 mA, which corresponded to a frequency shift of $\sim$ 10 MHz. The effect of this tuning technique can be seen in the locking cones of adjacent modes, the apparent variation in bifurcation position is due in fact to variation of the master/slave power ratio.

3. Free running QD-MLL

Without injection, the slave laser emitted pulses of $\sim$ 1.6 ps duration at the fundamental mode-locking frequency of 10.3 GHz with an optical spectral width of $\sim$5 nm at -10 dB and average power of $\sim$ 600 μW at 172 mA. Figure 2 shows the measured pulse shape and phase of the free-running laser (i.e. without optical injection) at -2.0 V absorber bias and 172 mA gain current. At gain currents below 200 mA the pulses emitted by the slave laser had a slightly asymmetrical shape with faster leading edge, and nearly-parabolic phase. Figure 2 shows the root-mean square fit (blue dashes) to the measured phase (red circles) assuming quadratic time dependence of the phase during the pulse, i.e. $\phi = at^2 + \phi_0$. The data can be fitted well with the parabola showing the linear pulse chirp with instantaneous frequency of $\nu = \frac{d\phi}{dt} = 2at$, with $a = 0.62(\frac{rad}{s^2})$. The laser exhibited a double pulse shape above a gain current of 200 mA and no pulse shape recovery was possible for the free-running laser at higher currents, similar to [8].

For experimental investigations the mode-locked regime with single asymmetric pulses was chosen (i.e. for the gain current below 200 mA, -2.0 V absorber bias). Optical and electronic spectra were measured for different current values at -2.0 V absorber bias. Laser threshold was

#173554 - $15.00 USD Received 2 Aug 2012; revised 28 Sep 2012; accepted 3 Oct 2012; published 25 Oct 2012

at 157 mA; in the region between 165 mA and 190 mA the laser exhibited stable mode-locking operation with clear RF signal at the fundamental mode-locking frequency and single pulses. Laser output was similar for all the currents in the range, therefore this region was chosen for the experimental study of injected laser dynamics. Optical and power spectra of the free-running mode-locked laser for this regime are shown in Fig. 3(a) and 3(b), respectively. The gain current change leading to a slave mode shift by a free spectral range (giving 10 GHz detuning between master and slave frequencies) was 10 mA; it corresponded to $\sim 6\%$ of the threshold current value, which meant to be remained in the same mode-locked regime despite the current tuning technique. Small changes in the gain and refractive index due to the current change can be neglected at least for a qualitative understanding of the bistability/hysteresis phenomenon.

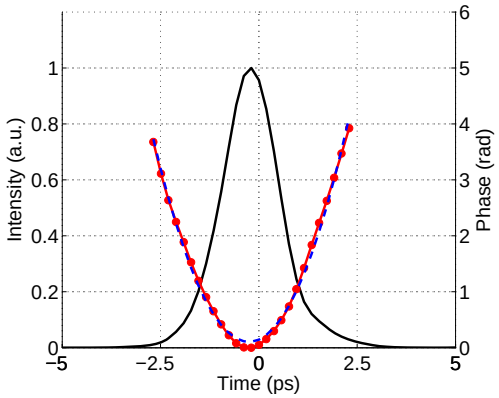

Fig. 2. Recovered pulse shape (black solid line) and phase (red circles) of the slave QD-MLL. The blue dashed line is the least squares parabolic fit of the phase. Absorber bias: −2.0 V, gain current: 172 mA.

4. Optical injection

Phase-locking of the QD-MLL to the CW master source (injected into the gain section) was indicated by a narrowing of the optical linewidth of the injected slave mode to that of the master; it was also accompanied by a significant narrowing of the slave laser optical spectrum and an increase of the mode-locking frequency [12, 13]. By varying master-slave detuning we experimentally identify three different regimes of operation in the optically injected MLL:

a) optical comb not locked to the injection:

The slave laser was mode-locked and not phase-locked to the master. There was a beating signal between the master and the slave fields observed in the RF spectrum. The frequency of the beating signal decreased as the slave mode approached the master frequency. When the injection was sufficiently far from the nearest slave longitudinal mode, the slave output characteristics were largely unaffected by the external forcing and were similar to the free-running case. The optical and RF spectra of the slave in this regime were essentially those of the free-running device, see Fig. 3(a) and 3(b).

b) optical comb is locked to the injection:

The laser became phase locked to the master laser, with no beating signal observed less than the mode spacing. The optical linewidth of the injected slave mode was narrow compared to the free-running value and reduced to that of the master laser (few hundred of kHz). Measured heterodyne beating signals of the slave mode with and without injection-locking are shown in Fig. 4. Only the modal linewidths in the vicinity of the injection were comparable to the master

#173554 - $15.00 USD Received 2 Aug 2012; revised 28 Sep 2012; accepted 3 Oct 2012; published 25 Oct 2012

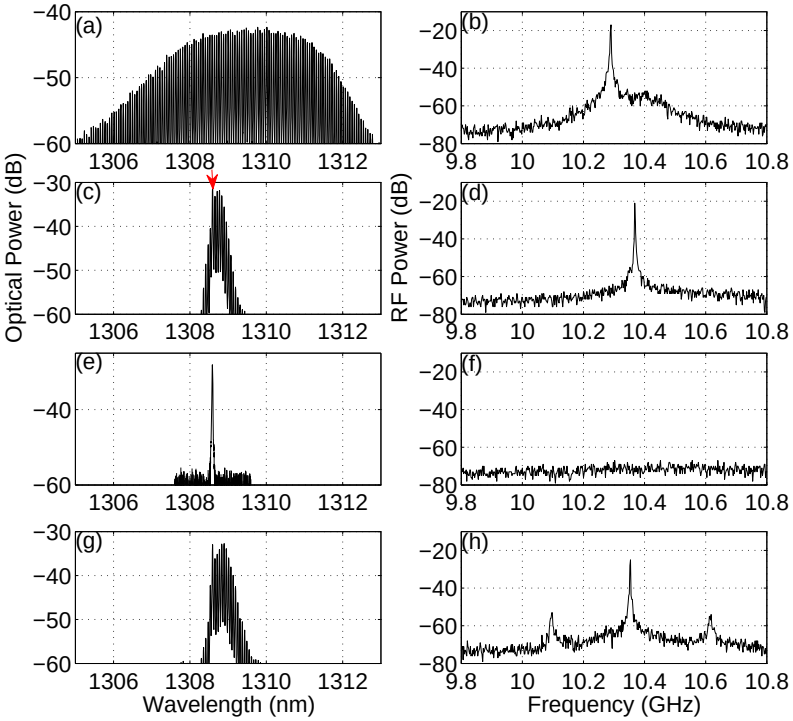

Fig. 3. Optical (a) and RF (b) spectra of the free running QD-MLL. Optical (c) and RF (d) spectra of the slave QD-MLL when it phase-locked to the injection seed. The injection seed indicated with an arrow is close to one of the slave modes. Optical (e) and RF (f) spectra of the injected QD-MLL when it operated in a single-mode regime. Optical (g) and RF (h) spectra of the slave QD-MLL in the bounded phase regime.

linewidth; as one moved away from the injection the linewidth significantly broadened [13].

The optical spectrum was narrowed and red-shifted from the injection wavelength as shown in Fig. 3(c). The mode-locking frequency was increased by the injection (see Fig. 3(d)). The magnitude of the shift was power dependent as has been previously shown [14].

c) single mode locked to the injection:

The slave laser was phase locked to the master and with only one mode lasing at the injection wavelength, as shown in Fig. 3(e). There was no signal at the mode-locking frequency (Fig. 3(f)). The single mode regime can be weakly modulated ($<$ 4 GHz, about the relaxation oscillation frequency).

5. Locking boundaries

The locking boundaries in an optically injected single mode laser model are formed by saddle-node and Andronov-Hopf bifurcations, both bifurcations well reproduce the observed experimental stability features [15]. The locking boundaries in our experiment are somewhat different, as might be expected with the multiple nonlinearly coupled oscillators being subject to injection.

We deduce the presence of the saddle-node bifurcation in our experiment through an abrupt transition from the unlocked to the locked regime, similar to the single-mode case. In the case of

#173554 - $15.00 USD Received 2 Aug 2012; revised 28 Sep 2012; accepted 3 Oct 2012; published 25 Oct 2012

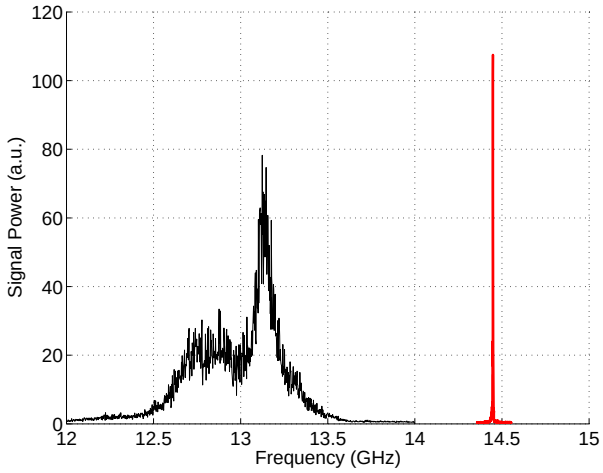

Fig. 4. Measured heterodyne beating signals of the slave mode with (red) and without (black) injection-locking. The slave mode was mixed with the TLS; the frequency of the TLS was adjusted so that the beating signal was in the area of $12-15$ GHz, in the region of the flat frequency response from detector and amplifier. Gain current: 172 mA; absorbr bias: -2.0 V; injection power: 35μW.

our mode-locked laser, it featured a sharp narrowing of the optical spectrum, and a substantial drop of the output power.

The other boundary was formed in a more complicated way as a gradual transition from the unlocked to the locked state. When the master signal frequency approached the slave modal frequency it resulted in a gradual narrowing of the slave optical spectrum (Fig. 3(g)), with the slave laser neither frequency locked nor phase locked at this stage. It was followed by a sharp narrowing of the modal linewidth of the nearest slave mode, due to phase locking to the master. The optical spectrum remained largely unchanged, but the RF spectrum contained low power sidebands for this regime, indicating a weak power modulation (Fig. 3(h)). The modulation frequency increased with the injection power from 100 MHz at an injection level of ~ 30 μW to 2 GHz at 750 μW. We propose that these weak power modulations result from bounded phase variations of the slave laser. Phase bounding is well known in optically injected lasers since the seminal work of Braza and Erneux [16], and has recently been experimentally examined in detail [17]. Finally, the phase of the injected mode of the slave laser was fixed to the master phase without visible modulations while the laser continued to generate short pulses.

According to [18], the appearance of the additional frequency in a single mode laser with external injection does not necessarily mean desynchronization. When the synchronized CW regime is destabilized via an Andronov-Hopf bifurcation, a regime with small periodic amplitude modulation is born. As long as the oscillating phase of the optical field is bounded, the average frequency coincides with the frequency ω_m of the external injection and, hence, the regime can be considered as synchronized to the frequency ω_m. When the modulation amplitude becomes sufficiently large, the phase starts to grow in time and the periodic regime becomes desynchronized. In this scenario the transition from the synchronized to desyncronized state is continuous and is not associated with any bifurcation. This single mode laser behavior is similar to that described experimentally above for the desynchronization of a periodic mode-locked regime, i.e. a bifurcation to a regime with a quasiperiodic laser intensity.

The multiple strongly coupled modes in our system lead to a rich variety of the dynamical

#173554 - $15.00 USD Received 2 Aug 2012; revised 28 Sep 2012; accepted 3 Oct 2012; published 25 Oct 2012

regimes which we discuss using a bifurcation diagram in the next section. The lower locking boundaries correspond to the abrupt transition to the locked state, and the upper boundaries were identified by the transition from the state with the bounded phase to the fully locked state.

6. Bifurcation diagram

We constructed a bifurcation diagram of the optically injected MLL in a two-parameter space: the master laser power, P_{inj}, and the detuning between master and slave frequency, $\Delta = \omega_m - \omega_s$. As discussed above, small variations in the slave drive current were made to ensure continuous sweeping of Δ. When the current was increased, the slave frequency ω_s decreased, and thus the detuning increased.

A schematic diagram of the regimes observed when the frequency ω_s was swept across an interval approximately two times larger than the cavity free spectral range is shown in Fig. 5 for Δ decrease (a), Δ increase (b) and both together (c). The upper boundaries of the regimes, denoted in the figure, were similar for both sweep directions, while the lower boundaries were significantly different for Δ increase and decrease, which resulted in regions with hysteresis as denoted in Fig. 5(c) by the cross-hatching. The measured diagrams overlain for both directions of the Δ sweep are shown in Fig. 6.

The bifurcation phenomena leading to locked/unlocked operation strongly depend on the injection power.

a) Low injection powers, $P_{inj} < P_s$ ($P_{inj} = 54\ \mu W$, $P_s = 600\ \mu W$, black vertical line in Fig. 6(b))

The power of the slave laser is plotted vs the detuning in Fig. 7(a). The blue curve corresponds to Δ decrease and the red curve corresponds to Δ increase. Figure 7(b) and 7(c) present corresponding diagrams of RF power spectra, showing beating between ω_s and ω_m vs Δ. As Δ was decreased the slave mode became locked to the master laser frequency at point *a* (see Fig. 7(b), Fig. 6(b), black line). The slave was locked between points *a* and *b*, with no instabilities observed, as shown in Fig. 7(b), and the laser unlocked below the point *b*. When the next slave mode became sufficiently close to the master (*c* in Fig. 7(b)), the slave was phased-locked until point *d*. For increasing Δ in contrast, there were no regions with proper locking of the slave laser, as shown in Fig. 7(c). The operating ranges $a-b$ and $c-d$ are thus bistable. A bistability between stable steady states and periodic regimes in optically injected distributed feedback QD lasers was recently described in [19].

b) Moderate injection powers, $P_{inj} \sim P_s$ ($P_{inj} = 745\ \mu W$, $P_s = 600\ \mu W$, blue vertical line in Fig. 6(b))

At moderate optical injection powers, regions with single-mode laser operation started to appear. Figure 8(a) shows the slave power vs detuning for Δ decrease (blue) and increase (red). Corresponding diagrams of low frequency spectra are presented in Fig. 8(b) and (d).

When Δ was decreased, between points $e(h)$ and $g(j)$ the slave laser was locked to the master, with no instabilities observed, as shown in Fig. 8(b). The gradual decrease of the output power and narrowing of the optical spectrum in this locked regime (Fig. 8(a)) eventually resulted in a single-mode operation regime between points $f(i)$ and $g(j)$ in Fig. 8(c). The single-mode regime was not detected for Δ increase at these injection powers. The locking ranges between points $k(l)$ and $h(e)$ were much smaller compared to the case of Δ decrease.

The locking boundaries are shown in Fig. 6. For Δ decrease the slave mode was locked from the blue side at the boundary *AH* (which includes points *c* and *h* in Fig. 6 and unlocked at the boundary *ABC* (which includes points *d* and *j* in Fig. 6). For Δ increase the laser was locked only at boundary *DE* and unlocked again at boundary *DH*.

The upper locking boundaries, *AH* and *DH*, were practically the same for both directions of

#173554 - $15.00 USD Received 2 Aug 2012; revised 28 Sep 2012; accepted 3 Oct 2012; published 25 Oct 2012

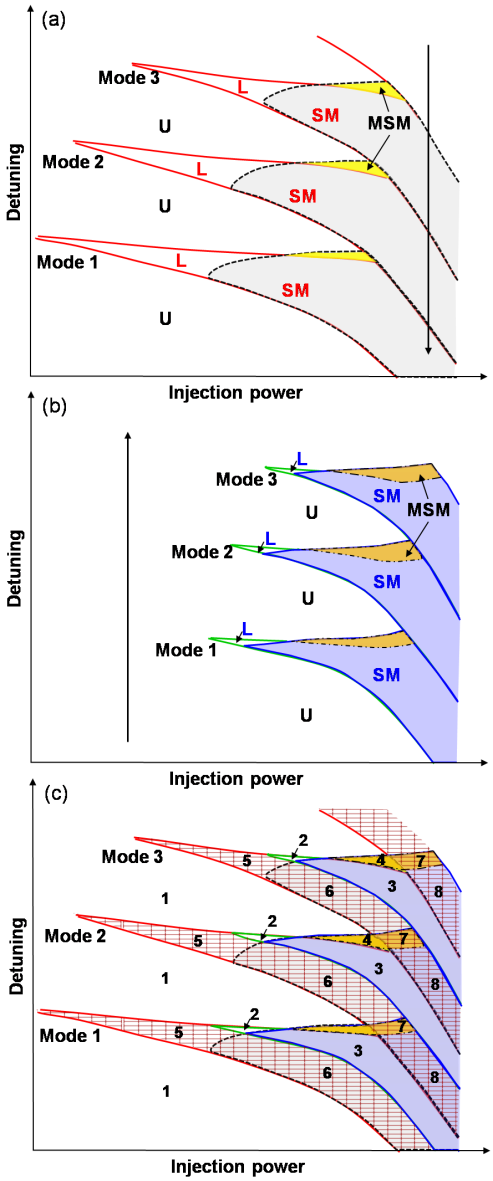

Fig. 5. Schematic representation of experimental data presented in Fig. 6. (a) corresponds to a decrease and (b) corresponds to an increase of Δ. Both maps are overlain in (c). The numbers and capital letters indicate the following regions: U: unlocked, L: Locked, SM: single-mode, MSM: modulated single-mode, 1: Unlocked, 2: Locked, 3: Single-mode, 4: Single-mode with modulation, 5: Unlocked or Locked bistable regime, 6: Unlocked or Single-mode bistable regime, 7: Single-mode 1 with modulation or Single-mode 2 bistable regime, 8: Single-mode 1 or Single-mode 2 bistable regime. The bistable regions are indicated with cross-hatching.

#173554 - $15.00 USD Received 2 Aug 2012; revised 28 Sep 2012; accepted 3 Oct 2012; published 25 Oct 2012

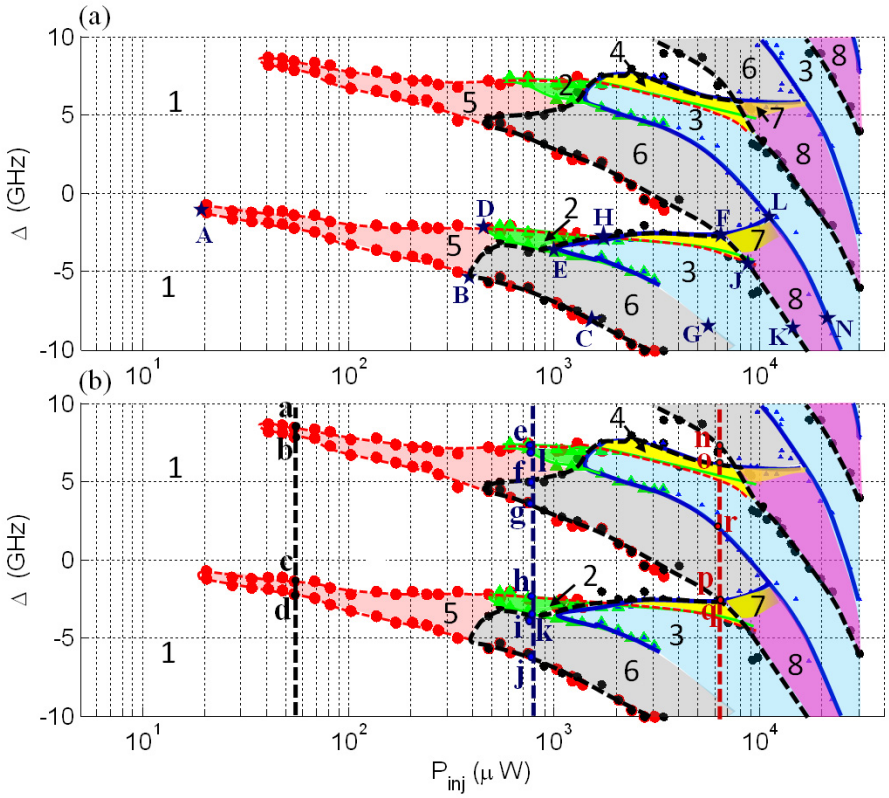

Fig. 6. Measured bifurcation diagram in two-parameter plane: master-slave detuning (ordinate) and master power (abscissa). Absorber bias: −2.0 V; gain current: 165 – 190 mA. (a) The numbers indicate the following regions: 1: Unlocked, 2: Locked, 3: Single-mode, 4: Single-mode with modulation, 5: Unlocked or Locked bistable regime, 6: Unlocked or Single-mode bistable regime, 7: Single-mode 1 with modulation or Single-mode 2 bistable regime, 8: Single-mode 1 or Single-mode 2 bistable regime. The capital blue letters with stars indicate the boundaries. (b) The dashed vertical lines and small letters indicate the points of transitions between different regimes for three different injection powers: 54 μW (black), 745 μW (blue) and 6.2 mW (red).

#173554 - $15.00 USD Received 2 Aug 2012; revised 28 Sep 2012; accepted 3 Oct 2012; published 25 Oct 2012

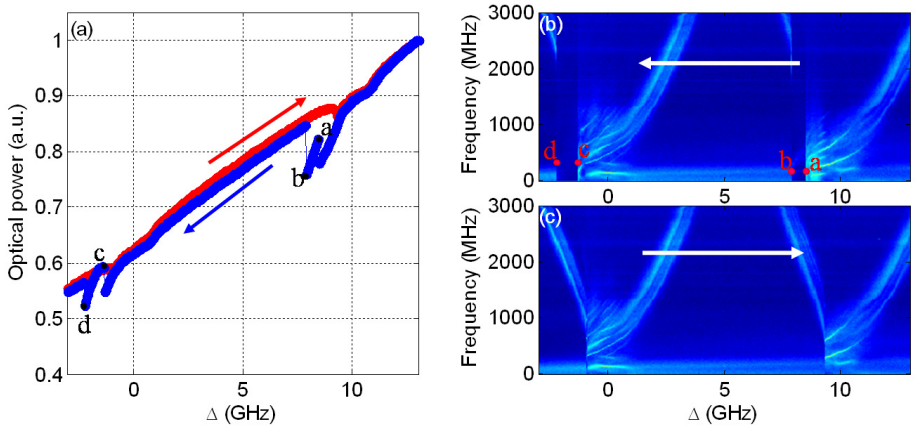

Fig. 7. (a) Slave power vs detuning for Δ decrease (blue) and increase (red). Low frequency spectrum vs detuning for decrease (b) and for increase (c) of Δ. Absorber bias: −2.0 V; gain current: 165 – 185 mA.

the master-slave detuning (see Fig. 6). The lower locking boundary was shifted from *ABC* for Δ decrease to *DE* for Δ increase resulting in the areas of bistability (regions 5 and 6 in Fig. 6).

The appearance of locked single mode operation at moderate injection powers thus gives another form of bistability, i.e. between the unlocked ML operation and locked single mode regime.

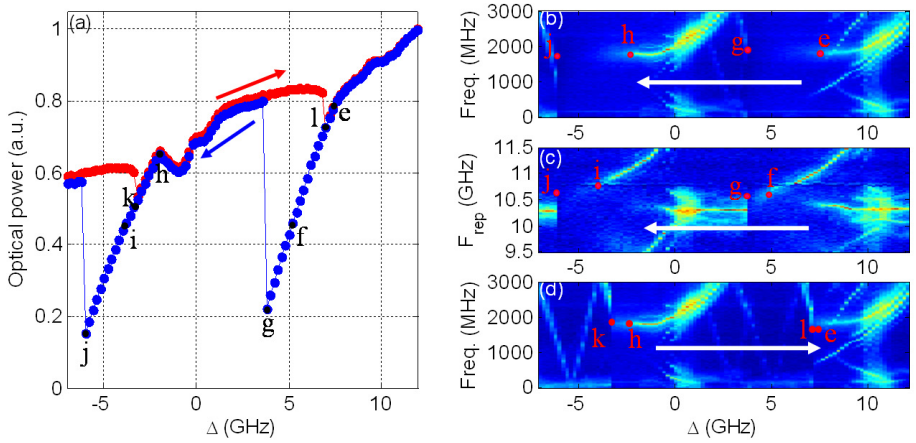

Fig. 8. (a) Slave power vs detuning for Δ decrease (blue) and increase (red). Low frequency spectrum vs detuning for decrease (b) and for increase (d) of Δ. Fundamental harmonic RF spectrum vs detuning for Δ decrease, (c). Absorber bias: −2.0 V; gain current: 165 – 185 mA.

c) High injection powers, $P_{inj} > P_s$ ($P_{inj} = 6200\ \mu W$, $P_s = 600\ \mu W$, red vertical line in Fig. 6(b))

At high injection powers, the regions of single-mode operation became significantly larger.

#173554 - $15.00 USD Received 2 Aug 2012; revised 28 Sep 2012; accepted 3 Oct 2012; published 25 Oct 2012

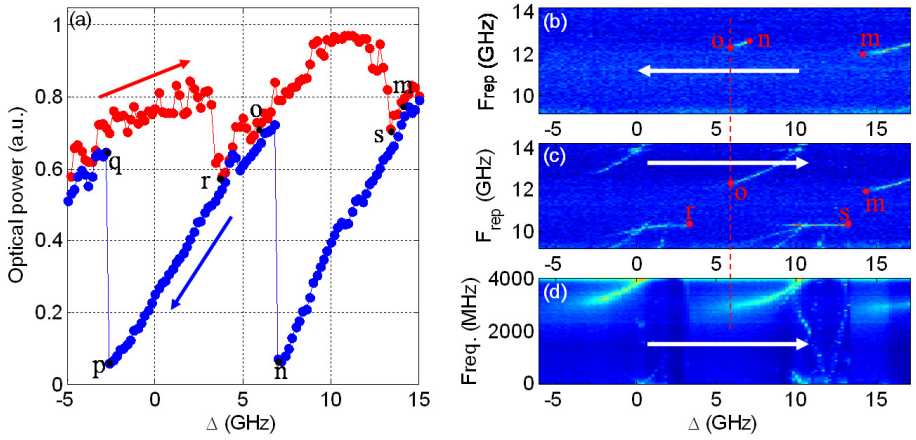

Fig. 9. (a) Slave power vs detuning for Δ decrease (blue) and increase (red). Fundamental harmonic RF spectrum vs detuning for decrease (b) and increase (c) of Δ. Low frequency spectrum vs detuning for Δ increase (d). Absorber bias: −2.0 V; gain current: 165 – 185 mA.

The slave laser operated in a single-mode regime within the black-dashed boundary *CBHF* for Δ decrease and within the blue boundary *GEHL* for Δ increase (see Fig. 6(a)).

The evolution of the RF spectra with detuning for Δ decrease is shown in Fig. 9(b). The slave laser operated in a single-mode regime between points *m* and *n*, and became single mode again below point *o*. For Δ increase the regions of single-mode operation were much smaller (between points *r* and *o*, and between points *s* and *m*), as shown in Fig. 9(c). The laser was unlocked between the intervals of single-mode behavior.

The upper boundaries of single-mode regimes (*BHF* and *EHF*) shown in Fig. 6, featured a gradual narrowing of slave laser optical spectrum. The laser characteristics changed abruptly at the lower boundaries of single-mode regime, *BC* and *EG*. These boundaries were different for Δ decrease (*BC*) and increase (*EG*) giving us bistability between single-mode and unlocked regimes (region 6 in Fig. 6(a)).

As the intervals of single-mode operation became larger, for certain parameters a weak modulation was seen as shown in Fig. 9(d). The regions of modulated single mode operation did not show any obvious bistability, as shown in Fig. 6, yellow areas. The modulation in the RF spectrum was gradually weakened with the increase of the injection power and could no longer be resolved for $P_{inj} > 9.6$ mW.

When the laser operated continuously single-mode, a transition between adjacent slave modes locked to the master was accompanied by an abrupt change in the laser power, see transition $p \rightarrow q$ in Fig. 9(a). These changes occurred at different detuning values for Δ decrease (*FK* boundary, see Fig. 6) and increase (*LN* boundary), indicating a new bistability between two single mode regimes (regions 7 and 8) with different powers, see Fig. 10(a-c). The effect of the detuning-induced switching between adjacent modes has previously been investigated for a single section semiconductor laser [20].

7. Hysteresis

The observed bistability led to a hysteresis in the laser output characteristics shown in Fig. 7(a) and Fig. 8(a) for low and moderate injection powers, respectively. The blue (red) line shows the

#173554 - $15.00 USD Received 2 Aug 2012; revised 28 Sep 2012; accepted 3 Oct 2012; published 25 Oct 2012

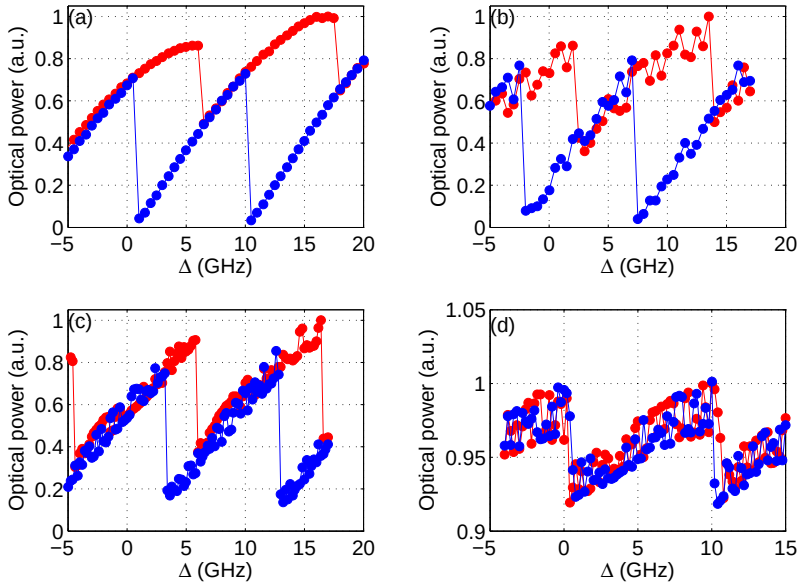

Fig. 10. Slave power vs master-slave detuning for Δ decrease (blue) and increase (red) at injection powers of 14 mW (a), 22.4 mW (b), 33 mW (c), and 120 mW (d). Absorber bias: −2.0 V; gain current: 165 – 190 mA.

slave laser power vs master-slave detuning for Δ decrease (increase). The area of the hysteresis loop increased with P_{inj} and saturated at moderate power injection. For higher injection power, the hysteresis area started to decrease and disappeared at ultra-high powers of 120 mW. Some examples of the hysteresis loop for a range of injection powers are shown in Fig. 10 for injection powers of 14 mW (a), 22.4 mW (b), 33 mW (c), and 120 mW (d).

8. Conclusion

For the first time we have constructed a two-parameter experimental bifurcation diagram of a QD-MLL under external CW optical injection. Four main laser operation regimes were identified in experiments and described: unlocked, locked, single mode, and single mode with modulation. We have determined the essential conditions for the optical comb being locked to the injection and revealed the bifurcation phenomena at the locking boundaries. Multiple hysteresis regions have been identified, which can potentially be utilized for wavelength switching and on-off power switching. The hysteresis regions initially grew with injection power and disappeared at the highest powers used in the experiment.

Acknowledgments

This work was funded by the EU FP7 Marie Curie Action FP7-PEOPLE-2010-ITN through the PROPHET project, Grant No. 264687, by the INSPIRE programme, funded by the Irish Government's Programme for Research in Third Level Institutions, Cycle 4, National Development Plan 2007-2013 and by Science Foundation Ireland under Contract No. 07/IN.1/I929. A.G.V. and A.P. acknowledge the support from SFB Project 787 of the DFG. A.G.V. was also supported by the Walton Visitor Award of the Science Foundation of Ireland and the program "Research and Pedagogical Cadre for Innovative Russia" (Grant No. 2011-1.5-503-002-038).

#173554 - $15.00 USD Received 2 Aug 2012; revised 28 Sep 2012; accepted 3 Oct 2012; published 25 Oct 2012